A mode-matching analysis of dielectric-filled resonant cavities coupled to terahertz parallel-plate waveguides

Victoria Astley,[1] Kimberly S. Reichel,[1] Jonathan Jones,[2] Rajind Mendis,[1] and Daniel M. Mittleman[1,*]

[1]*Department of Electrical and Computer Engineering, MS-378, Rice University, Houston, Texas 77005, USA*
[2]*Department of Electrical and Computer Engineering, Eastern Illinois University, Charleston, Illinois 61920, USA*
[*]*daniel@rice.edu*

Abstract: We use the mode-matching technique to study parallel-plate waveguide resonant cavities that are filled with a dielectric. We apply the generalized scattering matrix theory to calculate the power transmission through the waveguide-cavities. We compare the analytical results to experimental data to confirm the validity of this approach.

OCIS codes: (230.7370) Waveguides; (230.5750) Resonators; (300.6495) Spectroscopy, terahertz.

References and Links

1. H. Zhu, I. M. White, J. D. Suter, M. Zourob, and X. Fan, "Integrated refractive index optical ring resonator detector for capillary electrophoresis," Anal. Chem. **79**(3), 930–937 (2007).
2. T. Hasek, H. Kurt, D. S. Citrin, and M. Koch, "Photonic crystals for fluid sensing in the subterahertz range," Appl. Phys. Lett. **89**(17), 173508 (2006).
3. M. Loncar, A. Scherer, and Y. Qiu, "Photonic crystal laser sources for chemical detection," Appl. Phys. Lett. **82**(26), 4648–4650 (2003).
4. N. M. Hanumegowda, C. J. Stica, B. C. Patel, I. White, and X. Fan, "Refractometric sensors based on microsphere resonators," Appl. Phys. Lett. **87**(20), 201107 (2005).
5. B. You, J. Y. Lu, J. H. Liou, C. P. Yu, H. Z. Chen, T. A. Liu, and J. L. Peng, "Subwavelength film sensing based on terahertz anti-resonant reflecting hollow waveguides," Opt. Express **18**(18), 19353–19360 (2010).
6. S. Yoshida, E. Kato, K. Suizu, Y. Nakagomi, Y. Ogawa, and K. Kawase, "Terahertz sensing of thin poly(theylene terephthalate) film thickness using a metallic mesh," Appl. Phys. Express **2**(1), 012301 (2009).
7. C. Debus and P. H. Bolivar, "Frequency selective surfaces for high sensitivity terahertz sensing," Appl. Phys. Lett. **91**(18), 184102 (2007).
8. J. F. O'Hara, R. Singh, I. Brener, E. Smirnova, J. Han, A. J. Taylor, and W. Zhang, "Thin-film sensing with planar terahertz metamaterials: sensitivity and limitations," Opt. Express **16**(3), 1786–1795 (2008).
9. C. Rau, G. Torosyan, R. Beigang, and Kh. Nerkararyan, "Prism coupled terahertz waveguide sensor," Appl. Phys. Lett. **86**(21), 211119 (2005).
10. R. Mendis, V. Astley, J. Liu, and D. M. Mittleman, "Terahertz microfluidic sensor based on a parallel-plate waveguide resonant cavity," Appl. Phys. Lett. **95**(17), 171113 (2009).
11. V. Astley, K. Reichel, J. Jones, R. Mendis, and D. M. Mittleman, "Terahertz multichannel microfluidic sensor based on parallel-plate waveguide resonant cavities," Appl. Phys. Lett. **100**(23), 231108 (2012).
12. R. Mendis and D. M. Mittleman, "Comparison of the lowest-order transverse-electric (TE_1) and transverse-magnetic (TEM) modes of the parallel-plate waveguide for terahertz pulse applications," Opt. Express **17**(17), 14839–14850 (2009).
13. V. Astley, B. McCracken, R. Mendis, and D. M. Mittleman, "Analysis of rectangular resonant cavities in terahertz parallel-plate waveguides," Opt. Lett. **36**(8), 1452–1454 (2011).
14. A. L. Bingham and D. Grischkowsky, "High Q, one-dimensional terahertz photonic waveguides," Appl. Phys. Lett. **90**(9), 091105 (2007).
15. A. Bingham, "Propagation through terahertz waveguides with photonic crystal boundaries," Ph.D. Thesis, Oklahoma State University: Stillwater (2007).
16. P. P. Borsboom and H. J. Frankena, "Field analysis of two-dimensional integrated optical gratings," J. Opt. Soc. Am. B **12**(5), 1134–1141 (1995).
17. T. Thumvongskul and T. Shiozawa, "Reflection characteristics of a metallic waveguide grating with rectangular grooves as a frequency-selective reflector," Microw. Opt. Technol. Lett. **32**(6), 414–418 (2002).
18. T. Itoh, ed., *Numerical Techniques for Microwave and Millimeter-Wave Passive Structures* (Wiley, 1989).

#172172 - $15.00 USD Received 9 Jul 2012; revised 30 Aug 2012; accepted 31 Aug 2012; published 7 Sep 2012

19. R. Mendis and D. M. Mittleman, "An investigation of the lowest-order transverse-electric (TE_1) mode of the parallel-plate waveguide for THz pulse propagation," J. Opt. Soc. Am. B **26**(9), A6–A13 (2009).
20. C. A. Balanis, *Advanced Engineering Electromagnetics* (Wiley, 1989).
21. R. Mendis, "Nature of subpicosecond terahertz pulse propagation in practical dielectric-filled parallel-plate waveguides," Opt. Lett. **31**(17), 2643–2645 (2006).
22. J. P. Laib and D. M. Mittleman, "Temperature-dependent terahertz spectroscopy of liquid n-alkanes," J. Infrared Millim. Terahertz Waves **31**(9), 1015–1021 (2010).

1. Introduction

A research area of particular interest in recent years has been the use of resonant optical sensors as low-volume refractive index sensors. Refractive index sensing is noninvasive, simple to implement, does not require labels or chromophores for detection, and is sensitive to concentration rather than mass or volume, making it an ideal measurement technique for analyzing small volumes of analytes [1]. Resonant refractive index sensors measure the change in resonant behavior when an analyte is introduced to a system, either as a change in the extinction ratio or more frequently as a shift in the resonant frequency. Resonant sensors have been implemented with a wide range of geometries, such as optical ring resonators [1], photonic crystals [2,3], or microsphere resonators [4].

The majority of these designs operate at visible or infrared frequencies. At terahertz (THz) frequencies, refractive index sensing is less well developed. Many of the sensors such as dielectric-coated fibers, metallic meshes, and split-ring resonators have been implemented to sense thin dielectric layers, but the independent variable is the layer thickness rather than the index [5–8]. In contrast, other sensors in the THz range exist that are not sensitive to the layer thickness [9–11]. Further investigated here, the grooved parallel-plate waveguide (PPWG) design has been proposed as a high sensitivity sensor for monitoring the refractive index of the material filling the groove in both single-channel [10] and parallel multi-channel geometries [11].

In this approach, the resonant structure is a cavity integrated into a PPWG. A diagram is shown in Fig. 1. A rectangular groove is machined into the lower plate of the waveguide, which acts as a resonant cavity for THz radiation propagating inside the waveguide in the lowest-order transverse-electric (TE_1) mode [10]. We note that the more commonly employed TEM mode of the PPWG does not couple efficiently to a cavity of this type, so the use of the TE_1 mode is required [12]. This structure acts as a refractive index sensor; when the cavity is filled with a dielectric material, there is a corresponding change in the resonant frequency dependent on the material's refractive index [10]. In previous work we presented an application of mode-matching analysis to understanding the origin of the resonant behavior of the PPWG with an empty cavity [13]. In the work presented here, we expand this analysis to incorporate a dielectric filling in the cavity. This enables an analytical investigation of this waveguide's capability as a microfluidic sensor.

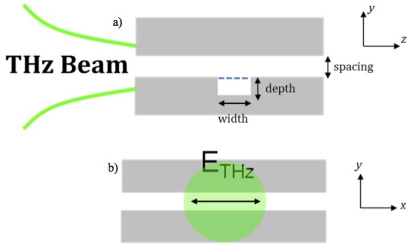

Fig. 1. Diagram of the grooved PPWG showing geometric parameters and the polarization and direction of the incident electric field. The dotted line indicates the (level of the) dielectric filling in the groove.

#172172 - $15.00 USD Received 9 Jul 2012; revised 30 Aug 2012; accepted 31 Aug 2012; published 7 Sep 2012

2. Mode-matching analysis

The mode-matching technique is a form of analysis employing classical waveguide theory and the generalized scattering matrix technique to analyze transmission through waveguides with discontinuous features such as abrupt changes in size, shape, junctions, cavities, etc [14–18]. The technique is discussed in detail in Ref [15] and in Chapters 9 and 10 of Ref [18]. In the case of a structure like the grooved waveguide under consideration here, the groove is treated as if it is a section of PPWG with a different plate separation and with its own supported modes. An incoming wave propagates through the ungrooved section, and then at the junction the wave is either transmitted into the various modes of the wider grooved section or reflected back into the ungrooved section. The transmitted waves propagate through the grooved section, before being transmitted or reflected at the junction with the second ungrooved section.

The amount of energy transferred across the (virtual) boundary from one mode to another by reflection or transmission depends on two factors: the impedance mismatch between the modes, and the amount of spatial overlap between the mode patterns. Modes with very similar electric field patterns will have a large spatial overlap and a correspondingly greater coupling efficiency, while modes with very different patterns will have a smaller overlap. If there is a large impedance mismatch at a boundary, energy is more likely to be reflected, while a small impedance mismatch leads to increased transmission.

This technique was used in Ref [13]. to analyze the empty-groove PPWG through the reflection and transmission of various TE modes at the start and end of the groove. The mode-matching technique has essentially the same form when applied to a waveguide with a dielectric-filled groove as to a waveguide with an empty groove: it calculates the reflection and transmission into various modes of the waveguide sections, based on the impedances and the overlap of the mode patterns. To incorporate a dielectric filling into the waveguide, those impedances and mode patterns must be recalculated to reflect the influence of the dielectric material on the field distribution inside the waveguide.

For the mode patterns and impedances in the ungrooved sections, we use the conventional equations for a TE-moded PPWG [19]. The grooved waveguide section can be treated as essentially a waveguide partially filled with a dielectric, and its mode patterns can be derived from those of a partially-filled rectangular waveguide. The mathematics of modes of a partially-filled rectangular waveguides are discussed in detail in Ref [20]. This analysis can be applied to derive the mode patterns of a partially-filled PPWG by extending the transverse dimension of the rectangular waveguide to infinity. This approach has been previously used to study THz pulse propagation behavior in partially-filled PPWGs [21]. After this extension to the PPWG geometry, the field patterns are described in each region by a set of TE components. Satisfying the boundary conditions of these regions yields a modified TE mode pattern. The resulting electric field distribution inside the dielectric-filled groove is given by:

$$E_x^d = \frac{-j\beta_Z A^d}{\varepsilon_d}\sin\left((\beta_{yd}(b-y)\right)e^{-j\beta_z z} \tag{1}$$

$$E_x^0 = \frac{-j\beta_z A^0}{\varepsilon_0}\sin(\beta_{y0}y)e^{-j\beta_Z Z} \tag{2}$$

where d indicates values in the dielectric and 0 indicates values in air, β is the propagation constant in the z or y directions, and the y-axis is defined with $y = 0$ at the top plate of the waveguide and $y = b$ at the bottom of the groove (Fig. 2). Here, x is the coordinate parallel to the air-dielectric interface. β_z in the propagation direction is the same in both the air and dielectric and must be determined numerically using the requirements for continuity of E_x and H_z at the dielectric-air interface. Both real and imaginary solutions must be found, as both

#172172 - $15.00 USD Received 9 Jul 2012; revised 30 Aug 2012; accepted 31 Aug 2012; published 7 Sep 2012

propagating and attenuating modes are considered in the mode-matching analysis. After solving for β_z, the electric field patterns for various modified TE modes can be plotted. Figure 2 shows typical patterns, in which the dielectric is assumed to be a non-absorbing liquid with a refractive index of n = 1.4224, which is the value for tetradecane at room temperature. The index is assumed to be real and independent of frequency, a reasonable approximation for many liquid hydrocarbons, which exhibit very low absorption and almost no dispersion in the THz range [22].

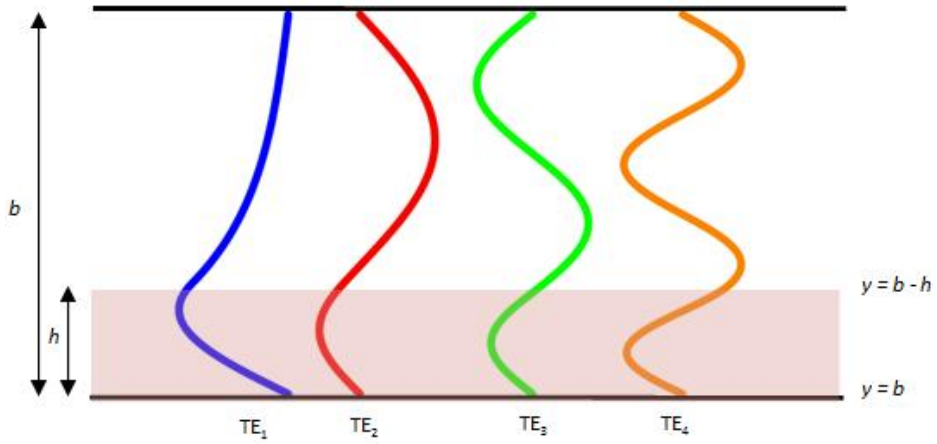

Fig. 2. Electric field patterns for the modified TE_1 to TE_4 modes of the partially dielectric-filled PPWG, illustrating the distortion of the mode due to the partial dielectric filling. The dielectric in this example is a slab of liquid (tetradecane) of height 412 μm, in a waveguide of total spacing b = 1.409 mm.

These modified mode patterns clearly show that the general shapes of the modes are similar to the ordinary sinusoidal TE modes of the empty waveguide, but there is a concentration of the propagating energy in the dielectric portion, as one might expect. The patterns above are calculated at 270 GHz. Unlike the modes of the empty waveguide, the modes of the partially-filled waveguide exhibit a frequency dependence even though the dielectric is assumed to have a frequency-independent refractive index. This effect is small and is due to the frequency dependence of the phase constant β_z. The modified TE mode patterns can be used in the mode-matching analysis to calculate the power transmission of various frequencies through the waveguide and thus the resonant frequency for empty or filled grooved PPWGs. These results can then be used to investigate the performance of the grooved PPWG as a microfluidic sensor. For example, a waveguide with a groove of dimensions 457 μm wide by 406 μm deep that is filled with materials with a wide range of refractive indices can be analyzed with the mode-matching technique to obtain a plot of the shift in the resonant frequency (Fig. 3). This analysis yields a quadratic dependence of the resonant shift on the index, as predicted by numerical simulations in previous work [10].

#172172 - $15.00 USD Received 9 Jul 2012; revised 30 Aug 2012; accepted 31 Aug 2012; published 7 Sep 2012

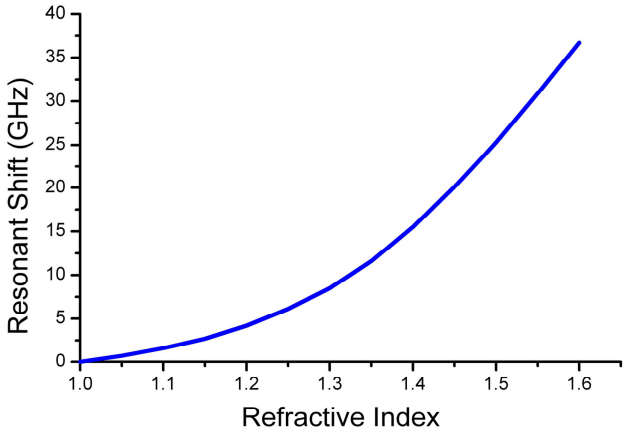

Fig. 3. Plot of the calculated shift in the resonant frequency for a groove of dimensions 457 μm by 406 μm when filled exactly to the top by dielectrics of varying refractive indices.

As an example of the value of the mode-matching technique, we consider the question of the dependence of the resonant frequency on the degree of filling of the cavity. In Fig. 3, the resonance shifts were calculated under the assumption that the groove is perfectly filled by the dielectric – a 406 μm column of liquid in a 406 μm deep groove. However, in reality, the filling level (*h* in Fig. 2 above) is an experimental variable. By starting with an empty groove and calculating the resonant frequency for the groove as it is slowly filled with a material (tetradecane, as in Fig. 2) at a series of fill heights from 0 μm to 406 μm, and continuing to overfill up to 500 μm, we can investigate the relationship between the fill height and the resonant shift [Fig. 4(a)]. This result can be used to calibrate the relationship between the fill height and the fluid volume in the groove, which is more easily controlled experimentally. Figure 4(b) is an example of an experimental curve relating the resonant shift to the volume of material introduced into the groove.

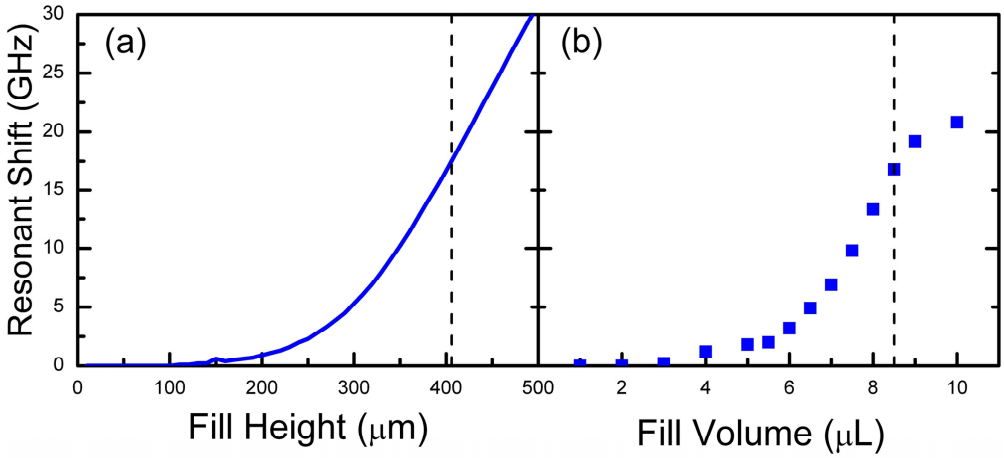

Fig. 4. Vertical dashed lines show a full groove filling. (a) Plot of the calculated shift in resonant frequency versus the height of the tetradecane filling in a 457 μm by 406 μm groove. A dashed line marks the height of a perfect fill, 406 μm. (b) Plots of the observed shift in the resonant frequency for a waveguide of the same geometry, as a function of the volume of liquid injected into the cavity, obtained experimentally.

The curve [Fig. 4(a)] indicates that there is a minimum fill height necessary to produce a measurable shift in the resonant frequency. It also indicates a roughly linear dependence on

#172172 - $15.00 USD Received 9 Jul 2012; revised 30 Aug 2012; accepted 31 Aug 2012; published 7 Sep 2012

fill height once this minimum level has been reached. This linear dependence continues beyond the point of perfect filling, which is experimentally unrealistic – as the experimental curve [Fig. 4(b)] shows, the groove begins to overflow at some point and the response saturates. Based on this saturated response and on visual observation of the fill, we can estimate the volume required to fill the groove (in this geometry 8.5 μL). The relationship between the height of the fill and the volume is nonlinear due to the experimental geometry, so there is no simple linear transformation between the analytical and experimental curves, but the two can be combined easily for calibration as described later in this paper.

Another curve that is useful for comparison to experiment is the dependence of the resonant shift on the plate spacing. In previous work we have demonstrated the dependence of the resonant frequency of the empty waveguide on the plate spacing [13]. It follows that the resonant frequency when the groove is filled would also depend on the spacing. However, mode-matching analysis allows us to easily determine whether the shift, the difference in those two resonant frequencies, also depends on the plate spacing. The result is plotted in Fig. 5 over the range of plate spacings for which the mode-matching technique has been shown to be accurate. For narrower plate spacings, the change is too abrupt between the grooved and ungrooved waveguide sections and the assumptions governing the mode-matching analysis are no longer valid [13]. We have used a plate separation of b = 0.997 mm for all mode-matching analysis, and a plate separation b = 0.99 mm ± 10 μm for all experimental data.

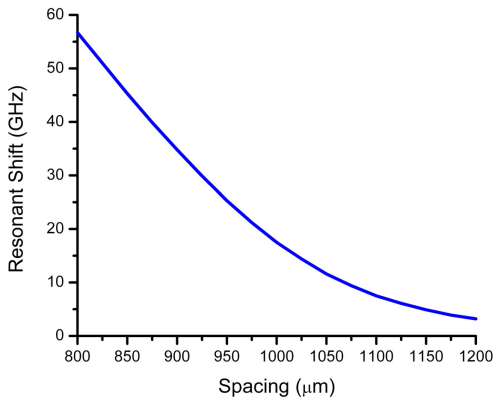

Fig. 5. The difference between the resonant frequency for the empty waveguide with the 457 μm by 406 μm groove, and the waveguide with the same groove filled with tetradecane, as a function of the spacing between the waveguide plates.

This figure demonstrates the importance of the accurate determination of the plate spacing, because it has a significant effect on the resonant shift observed for a particular refractive index. Higher shifts are observed for narrower waveguides than for waveguides with a wider spacing.

3. Comparison to experimental data and conclusion

To confirm the validity of this technique, we compare experimental results to the predictions from the mode-matching analysis. The experimental data discussed here have been published previously in Ref [11]. A parallel-plate microfluidic sensor was demonstrated with two independent grooves of dimensions 457 μm by 406 μm and 711 μm by 406 μm. As part of this demonstration, each channel was filled with a series of straight-chain alkanes (from octane to hexadecane) and the resonant shift for each sample was plotted versus the refractive index (blue squares and red circles in Fig. 6).

#172172 - $15.00 USD Received 9 Jul 2012; revised 30 Aug 2012; accepted 31 Aug 2012; published 7 Sep 2012

To reproduce this behavior analytically, we first model the empty waveguide to obtain the resonant frequency corresponding to each groove. Then we determine the height of the fill in each groove using graphs similar to Fig. 4. For example, a series of experiments filling the 457 μm by 406 μm groove with 8.5 μL of tetradecane yielded a resonant shift of 19 GHz. This corresponds to a fill height of 420 μm according to Fig. 4. The same procedure is done for the 711 μm by 406 μm groove, requiring a slight underfill of 350 μm to match the 34 GHz resonant shift observed for a 11.5 μL fill volume. These fill heights were then used in the mode-matching analysis to generate predictions of the resonant shift expected when the grooves were filled with these volumes of each of the other alkanes. These predicted shifts are plotted as straight lines in Fig. 6. The error bars in experimental data arise from variation of the liquid fill volume between trails. The largest source of error between experiment and analytic solution also arises from the liquid filling, both the consistency of the fill volume, and the varying characteristics among alkanes such as surface tension.

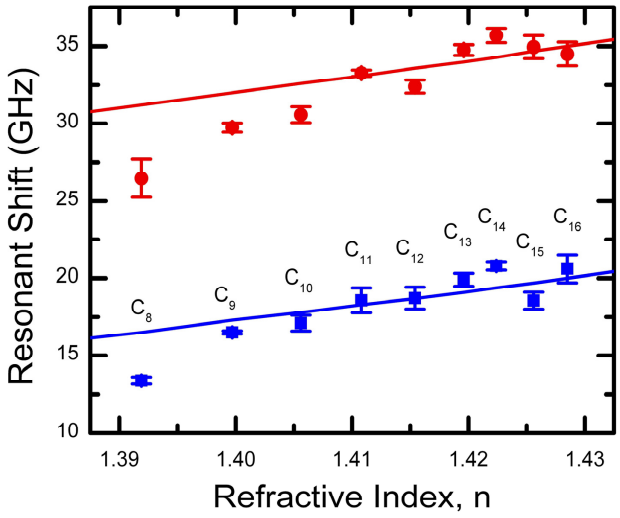

Fig. 6. Plot of the resonant shift (relative to the empty waveguide) obtained experimentally for a 711 μm by 406 μm groove filled to a height of 350 μm with a range of alkanes (red circles) and a 457 μm by 406 μm groove filled to a height of 420 μm with the same materials (blue squares). The lines are the predicted results from the mode-matching analysis.

The sensitivities predicted by the mode-matching analysis are slightly lower; 103 GHz/RIU for the 711 μm by 406 μm groove and 94 GHz/RIU for the 457 μm by 406 μm groove, than the experimental measurements of 225 and 170 GHz/RIU respectively obtained by a linear fit of the data. But the general trends agree reasonably well with the experimental data. This verifies the value of the mode matching technique for partially-dielectric-filled grooved PPWGs.

In conclusion, the technique presented here expands the mode-matching analysis to accurately describe the behavior of a grooved PPWG with a dielectric filling and thus provides a simple way to analyze and optimize this waveguide's capabilities as a microfluidic sensor.

Acknowledgments

This work has been funded in part by the National Science Foundation and by the Air Force Research Laboratory through the CONTACT program.

#172172 - $15.00 USD Received 9 Jul 2012; revised 30 Aug 2012; accepted 31 Aug 2012; published 7 Sep 2012